International Immunopharmacology 73 (2019) 81–93

Contents lists available at ScienceDirect

International Immunopharmacology

journal homepage: www.elsevier.com/locate/intimp

Time course study of oxidative stress in sulfur mustard analog 2-chloroethyl ethyl sulfide-induced toxicity

Mohsen Varmazyar[a], Zahra Kianmehr[b], Soghrat Faghihzadeh[c], Tooba Ghazanfari[d,*], Sussan Kaboudanian Ardestani[a,*]

[a] Institute of Biochemistry and Biophysics, University of Tehran, Tehran, Iran
[b] Department of Cellular and Molecular Biology (Biochemistry), Faculty of Biological Sciences, North Tehran Branch, Islamic Azad University, Tehran, Iran
[c] Biostatistics Department, School of Medicine, Zanjan University of Medical Sciences, Zanjan, Iran
[d] Immunoregulation Research Center, Shahed University, Tehran, Iran

ARTICLE INFO

Keywords:
Oxidative stress
Sulfur mustard
CEES
Toxicity
Time course changes
Mice

ABSTRACT

Oxidative stress is the major mechanism impairing cell homeostasis, inducing cell death and tissue damage in sulfur mustard (SM)-exposed individuals. The aim of the present study was to evaluate time course changes of oxidative stress in the mice exposed with 2-chloroethyl ethyl sulfide (CEES) as SM analog. For this purpose, male BALB/c mice were divided into control groups and experimental groups that received CEES (10 mg/kg) through intraperitoneal injection. In both groups, animals were euthanized at three periods: short (12, 24 h and 1 week), medium (1, 2 and 3 months) and long-term (5 and 6 months) after CEES exposure. Oxidative stress indices and the antioxidant defense systems were evaluated in lung and liver tissues. The time course findings in both tissues showed a significant increase in oxidative damage markers such as malondialdehyde (lung $P < 0.001$, liver $P < 0.001$), protein carbonyl (lung $P < 0.0001$), and 8-hydroxy-deoxyguanosine (lung $P < 0.0001$, Liver $P < 0.0001$) and also a significant reduction in the antioxidant defense system including reduced glutathione level (lung $P < 0.001$, Liver $P < 0.001$,), activities of catalase (lung $P < 0.01$ and liver $P < 0.05$), superoxide dismutase (lung $P < 0.05$), glutathione S-transferase (lung $P < 0.05$, liver $P < 0.01$), glutathione peroxidase (lung, $P < 0.05$, Liver $P < 0.05$) and glutathione reductase (lung $P < 0.001$, liver $P < 0.01$) in the long-term. However, these changes occur with less intensity in the short-term and return to the normal status in the medium-term. Moreover, there was a positive time course correlation between oxidative damage indices and the percent of histopathological damage in both tissues ($P < 0.05$). This correlation finding confirms and supports the fact that time course oxidative-antioxidant imbalance plays an important role in the development of SM-induced acute and delayed injuries.

1. Introduction

In the biological systems, numerous endogenous and exogenous sources can generate a variety of reactive oxygen species (ROS) [1]. ROS plays functional roles in physiological and pathological conditions depending on the cell capability to maintain the balance between the ratio of ROS production and its clearance. [2,3]. The cellular antioxidant defense system, including enzymatic and non-enzymatic counterparts, ensures the balance between ROS production and elimination. Enzymatic antioxidant defenses include superoxide dismutase (SOD), catalase (CAT), glutathione reductase (GR), glutathione peroxidase (GPX) and glutathione S-transferase (GST). Non-enzymatic antioxidants consist of reduced glutathione (GSH), natural flavonoids, carotenoids, melatonin and Vitamins A, C, and E [1].

Oxidative stress is a status characterized by the imbalance toward the pro-oxidant side of the pro-oxidant/antioxidant homeostasis caused by overproduction of ROS or declined antioxidant capacity [2–4]. This phenomenon leads to oxidative damage to many molecules in cells including nucleic acids, proteins, and lipids which can modify their structure and function [4,5]. A considerable number of studies have confirmed that oxidative stress is an underlying mechanism in different pathologies including chronic inflammatory diseases, multiple sclerosis, neurodegenerative diseases, cardiovascular diseases, diabetes, atherosclerosis, aging, cancer, the toxicity associated to heavy metals [1,6–10], and the complications triggered by sulfur mustard exposure [11–15].

* Corresponding authors.
E-mail addresses: ghazanfari@shahed.ac.ir (T. Ghazanfari), ardestany@ut.ac.ir (S.K. Ardestani).

https://doi.org/10.1016/j.intimp.2019.04.055
Received 5 February 2019; Received in revised form 19 April 2019; Accepted 25 April 2019
Available online 10 May 2019

Sulfur mustard (SM, bis (2-chloroethyl) sulfide) is a vesicant and cytotoxic alkylating agent with known mutagenic and carcinogenic properties [12]. It has been used as a chemical warfare agent in a number of conflicts such as the Iran–Iraq war (1980–1988) in which about 100,000 Iranian people were injured due to this agent, and even after more than two decades about 34,000 of them are still under treatment [16,17].

The severity of SM-induced complications mainly depends on the dose, duration, and environment of SM exposure [18,19]. SM exposure may cause short and long-term adverse health effects in many organs especially the skin, eyes, and respiratory system [20]. Short-term (early) complications occur in the first week following exposure, but long-term (delayed) complications may appear even some months or years after the exposure and have a serious impact on the life quality of the exposed individuals [21,22].

Respiratory complications are among the most frequent and important causes of long-term disability and mortality in SM-exposed individuals [23,24]. Some cellular and molecular mechanisms have been introduced to explain the toxicological effects of SM, but the exact mechanism is unclear [25]. Many investigations have been trying to determine the pathophysiological and molecular mechanisms underlying the short and long-term effects of SM as well as changes occurring in biomarkers of oxidative stress after SM exposure in different study models [26–30]. However, detailed information about SM toxicity in human, especially in the lung, is incomplete due to the difficulties of lung tissue sampling. Since, the lungs of these patients are very sensitive to invasive sampling methods (surgery, bronchoscopy) and the risk of bleeding, heart arrest, and bronchial spasm is high. Thus, most of the previous studies have evaluated desired parameters in blood or bronchoalveolar lavage (BAL) fluids in SM-exposed patients rather than lung tissue sampling [31–33]. To overcome this problem, animal models can be considered as alternative sources for obtaining comprehensive information about the molecular mechanisms of SM toxicity and examining possible therapeutic approaches for improving the life quality of SM-exposed victims.

The time course studies are used to examine single dose toxicity of substances and to evaluate drug therapy and drug response in various diseases [34–38]. In this regard, several animal studies using SM or its analogs such as CEES (2-chloroethyl ethyl sulfide) have evaluated the short, medium, or rarely long-term complications of SM in special target organs [29,39,40]. However, there was no special animal model that exactly simulated the development of SM injury in human from the short-term to the long-term condition. In addition, there are no time course studies to clarify the molecular mechanisms underlying the short and long-term effects of SM. In our previous study, different parameters consisting mice strain (BALB/c and C57BL/6), the period after exposure (12 h to 6 months), solvents (Tyrode's, PEG300, herbal oil), and CEES dose (1–200 mg/kg) were evaluated to create an animal model of SM-exposed victims. Mortality rate assessments and pathological findings revealed that intraperitoneal injection of 10 mg/kg CEES in herbal oil to BALB/c mice could develop a proper model which almost imitates short and long-term complications of SM exposure in humans [41].

The present study aimed to provide an overview of the time course changes in oxidative stress induced by CEES exposure, thus, helping to shed light on the molecular mechanisms of the damage caused by mustard gas. To achieve this purpose, the important indices of oxidative damage including malondialdehyde (MDA), protein carbonyl (PCO), 8-hydroxy-deoxyguanosine (8-OHdG) were evaluated in lung and liver tissues of the developed animal model. Besides, antioxidant defense parameters consisting of oxidized and reduced glutathione level, activities of CAT, SOD, GR, GPX, and GST were evaluated. The time course findings of this study might be helpful for the clinical management of the SM-induced disorders and for the selection of appropriate treatment at the right time.

2. Materials and methods

2.1. Chemicals

TBA (thiobarbituric acid), BHT (2,6-di-tert-butyl-4-methylphenol), DNPH (dinitrophenyl hydrazine), streptomycin sulphate, TCA (trichloroacetic acid), ethanol, ethylacetate, HCl (hydrochloride acid), hydrogen peroxide (H_2O_2), guanidine hydrochloride, xylenol orange, hydrogen peroxide, ABTS (2,2′-azino-bis(3-ethylbenzothiazoline-6-sulfonic acid), Trolox, NADPH (nicotinamide adenine dinucleotide phosphate), GSH (reduced glutathione), GSSG (oxidized glutathione), glutathione reductase, DTNB (5,5-dithiobis 2-nitrobenzoic acid), 2-vinilpyridine, CDNB (1-chloro-2, 4-dinitrobenzene), WST-1 (sodium salt of 4-[3-(4iodophenyl)-2-(4-nitrophenyl)-2H-5-tetrazolio]-1,3-benzene disulfonate), Hypoxanthine, DTPA (diethylenetriamine-pentaacetic acid), SOD (Cu/Zn superoxide dismutase), BSA (bovine serum albumin), PMSF (Phenylmethanesulfonyl fluoride), and EDTA (Ethylenediaminetetraacetic acid) were purchased from Sigma and Merck Companies.

2.2. Animals

6–8 week-old male BALB/c mice (20–25 g) were purchased from a breeding stock kept at the Pastor Institute (Karaj, Iran) and put under standard conditions in the animal house of the Institute of Biochemistry and Biophysics, University of Tehran. All animal experiments and methods were conducted according to the guidelines of the Animal Ethics Committee of the University of Tehran. Mice were housed in cages in a ventilated room with free access to food and water at a controlled temperature of 20 ± 2 °C, and maintained under a normal light-dark cycle.

2.3. Median lethal dose (LD50) of CEES in BALB/c mice

For the determination of LD50, 5 log doses and for each dose, 4 animals were used. The body weights were recorded daily and the animals were observed for mortality. LD50 was determined in the mice after dissolving CEES in herbal oil and intraperitoneal injection of different doses (10–30 mg/kg). The mortality was recorded for a 14-day period and the LD50 was determined as per the moving averages method [42].

2.4. Animal exposure with CEES

In experimental groups, BALB/c mice were injected intraperitoneally with single doses of 100 μL CEES 10 mg/kg (~0.5LD50) in herbal oil. Control animals were injected with herbal oil in the same way. At the time of these injections, all of the personal and environmental protection protocols set by the CEES manufacturer including the use of a chemical mask and gloves, dressing gowns, and the laminar flow hood with the charcoal filter was followed. Animals from both control ($n = 5$) and experimental ($n = 7$) groups were euthanized in a time-dependent manner as shown in Table 1: 12, 24 h (h); 1, 2 weeks (w) and 1, 2, 3, 4, 5 and 6 months (m) after CEES exposure and then samples from the liver and lung tissues were collected.

Table 1
Classification of the mice groups based on euthanized time after injection.

Groups	Short-term				Medium-term				Long-term	
Time after injection	12 h	24 h	1 week	2 weeks	1 month	2 months	3 months	4 months	5 months	6 months

As described, respiratory problems are the greatest cause of long-term disability in victims even 30 years after initial exposure to mustard gas [23,24]. Therefore, the current study period was performed during 6 months, which is consistent with age mapping data between humans and mice about lung disease [43]. To analyze the results carefully, time point groups were categorized to the three durations: short, medium and long-term and two weeks; the fourth month in these time groups were ignored for setting the gap between them.

2.5. Tissue preparation

The mice in the different groups were sacrificed and liver and lung quickly removed, washed in ice-cold phosphate buffer saline (PBS). Specimens from each organ was immediately immersed in liquid nitrogen and stored at −70 °C until biochemical analysis. The frozen tissue samples were quickly weighed and separately homogenized 1:5 in ice-cold 50 mM potassium phosphate buffer (pH ~ 7.4) containing 1 mM EDTA and 100 mM PMSF with a potter-Elvenhjem tissue homogenizer. The crude tissue homogenates were centrifuged at 12000 ×*g* for 15 min at 4 °C. The resultant supernatants were separated and used for the different assays.

2.6. Malondialdehyde (MDA) measurement

Lipid peroxidation levels were measured according to Ohkawa et al. method [44]. This assay depends on the reaction of TBA with MDA as the end product of lipid peroxidation. The pink chromogen produced by this reaction was measured at 532 nm. MDA concentration was expressed in nmol of MDA/g wet tissue (nM/gwt) using the extinction coefficient of 156 $mM^{-1}\,cm^{-1}$.

2.7. Protein carbonyl (PCO) measurement

PCO content was determined by the colorimetric method [45,46] with some modifications. This method is dependent on a Schiff base forming from DNPH reacting with protein carbonyls for protein hydrazones formation. Briefly, following the treatment of the samples with streptomycin sulfate for removing any nucleic acids, each sample was divided into two aliquots. DNPH in 2.5 M HCl was added to one aliquot and 2.5 M HC1 to the other as a control blank. After precipitation of protein with TCA and washing procedure with 1:1 ethanol-ethylacetate, the final palette was dissolved in 6 M guanidine hydrochloride. PCO level was determined from the absorbance at 370 nm and calculated from the molar absorption coefficient of 22,000 $M^{-1}\,cm^{-1}$. The result was expressed as nmol carbonyl/mg protein (nM/mg).

2.8. DNA oxidation measurement

Tissue homogenate level of 8-hydroxy-deoxyguanosine (8-OHdG) as a marker for DNA oxidation was measured using a commercial 8-OHdG ELISA Kit (My BioSource, MBS263767, USA) according to the manufacturer's instructions. 8-OHdG concentration was reported in ng/ml. The level of sensitivity of the kit was 50.0 pg 8-OHdG/ml.

2.9. Total oxidant status (TOS) measurement

TOS levels of tissue homogenate were determined using xylenol orange as a reactive dye and hydrogen peroxide as a standard [47,48]. In this method, oxidants present in the sample oxidize Fe^{2+} to Fe^{3+}. The absorbance of the purplish color complex produced by the reaction of Fe^{3+} with xylenol orange was measured at 580 nm. The assay was calibrated with hydrogen peroxide, and the results were expressed in terms of micromolar hydrogen peroxide equivalent per gr wet tissue (μmol H_2O_2 Eq/g wet tissue).

2.10. Total antioxidant capacity (TAC) measurement

TAC levels of tissue homogenate were determined according to the technique described by Re et al. [49]. This assay is a functional marker of the non-enzymatic antioxidant capacity of a sample in which, the blue/green color of ABTS radical cation ($ABTS^{\cdot+}$) is bleached by antioxidants present in the sample. The rate of decolorization expressed as a percentage inhibition of $ABTS^{\cdot+}$ and quantified relative to the reactivity of Trolox as a standard curve. The assay results are expressed in μmol Trolox Eq/g wet tissue.

2.11. Oxidative stress index (OSI) measurement

Oxidative stress index (OSI), as an indicator of the degree of oxidative stress, is the ratio of the total peroxide to the total antioxidant potential. The OSI value was calculated by the following formula [50]:

$$OSI = [(TOS, \mu mol\ H_2O_2\ Eq/g\ wet\ tissue)/(TAC, \mu mol\ Trolox\ Eq/gr\ wet\ tissue)]$$

2.12. Oxidized, reduced and redox ratio glutathione measurement

The estimation of oxidized and reduced glutathione level was assessed according to the method of Griffith and Tietze [51,52]. Tissue extracts and GSH standard were prepared in ice-cold 5% w:v metaphosphoric acid to keep the glutathione values stable. Total glutathione content was determined by following the rate of reduction of DTNB by reduced glutathione in the coupled reaction with glutathione reductase at 412 nm and compared with a GSH standard curve [52]. The GSSG level was measured by the same method in tissue extracts that were pre-incubated with 2-vinylpyridine to bind GSH [51] Total glutathione was defined as GSH-equivalents (GSH-eq) [GSH-eq = GSH + 2 GSSG]. Therefore, GSH content was calculated by subtracting GSSG levels from the total glutathione content. The glutathione redox ratio (GRR %) as an index of oxidative stress was calculated according to the formula [53]: $GRR\% = [GSSG / (GSH + GSSG)] \times 100$.

2.13. Catalase (CAT) activity assay

CAT activity was determined according to the method of Aebi [54]. This assay is based on measuring the rate of decrease in H_2O_2 absorbance at 240 nm. CAT activity was expressed as μmol/min/mg protein using a molar extinction coefficient of H_2O_2 ($\varepsilon = 0.0436\ mM^{-1}\,cm^{-1}$).

2.14. Superoxide dismutase (SOD) activity assay

SOD activity was assayed according to the method of Peskin and Winterbourn [55]. In this assay, the reduction rate of WST-1, water-soluble tetrazolium salt as a superoxide detector, was measured at 450 nm. Results were expressed as the percentage of inhibition of the formazan salt formation that is in inverse relation to SOD activity. The SOD activity was calculated by the SOD logarithmic standard curve.

2.15. Glutathione S-transferase (GST) activity assay

GST activity was assayed by the method of Habig et al. adapted to a microplate reader [56]. This assay monitored the formation of the dinitrophenyl thioether product of the reaction between GSH and CDNB at 340 nm. GST activity was expressed as μmol/min/mg protein using a molar extinction coefficient of CDNB ($\varepsilon = 9.6\ mM^{-1}\,cm^{-1}$).

2.16. Glutathione peroxidase (GPX) activity assay

GPX activity was assayed by a modified method of Flohé and Günzler adapted for use in a microplate reader [57]. This activity was

determined with H_2O_2 as substrate and GR and NADPH as enzyme and non-enzymatic indicators, respectively. The GSSG generated by GPX of the sample was reduced by GR, and NADPH oxidation was monitored at 340 nm. GPX activity was expressed as μmol/min/mg protein using a molar extinction coefficient of NADPH ($\varepsilon = 6.22\,mM^{-1}\,cm^{-1}$).

2.17. Glutathione reductase (GR) activity assay

GR activity was measured in accordance with an adaptation of the microplate method described by Cribb et al. [58]. In this assay, GR of the sample generated GSH from the added GSSG to the reaction, and then GSH caused the reduction of DTNB. The reduction of DTNB was monitored at 412 nm, and the rate of the increase in absorbance was directly proportional to the amount of GR in the sample. GR activity was expressed as μmol/min/mg protein using a molar extinction coefficient of DTNB ($\varepsilon = 14.15\,mM^{-1}\,cm^{-1}$).

2.18. Determination of protein content

Protein content in tissue homogenates was measured according to the Bradford method using BSA as standard [59].

2.19. Statistical analysis

Values of the measured parameters were expressed as mean ± SD. The difference between the control and treated groups were determined using the unpaired student's *t*-test. One-way ANOVA followed by Tukey test was used for comparisons of time groups. *P*-values < 0.05 were considered statistically significant. Pearson's correlation coefficient with the significant level < 0.05 was used to explore the correlation between variables. All calculations were performed using Excel 2016 and GraphPad InStat Version 7.

3. Results

3.1. Details of determining the appropriate dose to create the animal model

Details of changes in mortality rate, animals body weight and pathological findings in lung and liver tissues of BALB/c and C57BL/6 mice receiving different CEES doses with variable solvents from 12 h to 6 months after CEES injection were presented in our previous study [41] and a summary of these results is listed below.

The LD50 dose of CEES in herbal oil was determined at 17.5 mg/kg. Pathological features detected in BALB/c mice were more severe than the C57BL/6 mice. In addition, the dose of 10 mg/kg CEES (~half of LD_{50}) in herbal oil induced a high weight loss, the lowest mortality rate, and the highest pathological complications. Therefore, BALB/c mice and the dose of 10 mg/kg CEES in herbal oil were selected to study the short-term and long-term complications following exposure to SM. The short and long-term pathological changes after CEES injection are shown in Table 2.

The complications were categorized into two modes, time-dependent and independent. Time-independent are the short-term pathological complications that occurred 12 h after contamination with CEES and continued by the end of the sixth month. Severe pathological signs are time-dependent that occurred after 4 months (long-term).

The Gross view of lung morphology changes in lung and liver tissues occurred in long-term after CEES exposure are illustrated in Fig. 1. Moreover, the related pathological alteration of the lung tissue in long-term are presented in the previous study in detail [41].

3.2. The time course change of MDA, PCO and 8-OHdG levels in lung and liver tissues of CEES-exposed mice

As shown in Fig. 2.A, the CEES-induced oxidative shock has increased the MDA levels (nM/gwt) of the lung and liver in the short-term (12 and 24 h), but this increase is not significant. MDA levels of the lung and liver within 5 (lung 134.02 ± 6.21, $P < 0.05$ and liver 85.03 ± 14.98, $P < 0.05$) and 6 months (lung 137.99 ± 17.31, $P < 0.05$ and liver 95.52 ± 12.12, $P < 0.05$) increased significantly compared to their respective control groups (lung 113.11 ± 19.85, 112.55 ± 11.58, and liver 62.49 ± 3.99, 77.55 ± 14.89 respectively) (Fig. 2.A linear graph, Table 4). In both tissues MDA levels were almost stable at the medium-term group, while MDA levels in long-term (lung 136.16 ± 13.03, $P < 0.001$ and liver 90.66 ± 14.02, $P < 0.001$) increased significantly compared to the control (lung 112.83 ± 15.31 and liver 70.04 ± 8.09), short (lung $P < 0.01$, liver $P < 0.0001$) and medium-term groups (lung $P < 0.0001$, liver $P < 0.0001$) (Fig. 2.A bar graph).

The level of PCO (nM/mg) was significantly increased in the lung within 2 (2.13 ± 0.31, $P < 0.05$), 5 (2.7 ± 0.37, $P < 0.01$) and 6 months (2.63 ± 0.37, $P < 0.001$), as well as within 24 h (2.56 ± 0.2, $P < 0.01$) in the liver compared to their respective control groups (Lung 1.74 ± 0.27, 1.98 ± 0.26, 1.62 ± 0.08, and liver 2.22 ± 0.13, respectively) (Fig. 2.B. linear graph, Table 4). Lung of mice showed a significant increase in PCO content within medium (2.24 ± 0.4, $P < 0.05$) and long-term periods (2.67 ± 0.35, $P < 0.0001$) in comparison with their respective control groups (1.93 ± 0.37, 1.8 ± 0.26, respectively) and in medium ($P < 0.001$) and long-term ($P < 0.0001$) vs. short-term group and long-term ($P < 0.0001$) vs. medium-term group. While no significant change was found in the liver between different groups (Fig. 2.B bar graph).

Lung 8-OHdG level (ng/mg) within 12 h (1.21 ± 0.104, $P < 0.05$), 2 (1.12 ± 0.091, $P < 0.05$), 5 (1.32 ± 0.114, $P < 0.01$) and 6 months (1.28 ± 0.118, $P < 0.01$) were significantly higher as compared to their respective control groups (1.04 ± 0.111, 0.96 ± 0.112, 0.99 ± 0.101 and 0.932 ± 0.159, respectively) also in the liver within 24 h (5.096 ± 0.22, $P < 0.001$), 1 week (5.33 ± 0.27, $P < 0.05$), 5 (5.9 ± 0.167, $P < 0.001$) and 6 months (5.156 ± 0.388, $P < 0.01$) were significantly higher compared to their respective control groups (3.78 ± 0.194, 4.64 ± 0.531, 4.292 ± 0.295, 4.4 ± 0.227, respectively) (Fig. 2.C linear graph, Table 4). The significant increase in lung 8-OHdG content in the medium (1.13 ± 0.121, $P < 0.01$) and long-term groups (1.304 ± 0.110, $P < 0.0001$) was observed compared with their respective control groups (1.012 ± 0.090, 0.961 ± 0.129, respectively) and long-term than short ($P < 0.0001$) and medium-term ($P < 0.001$) groups. In liver, there was a significant increase in the 8-OHdG content of short (4.74 ± 0.727, $P < 0.05$) and long-term periods (5.53 ± 0.482, $P < 0.0001$) compared to their respective control group (4.157 ± 0.486, 4.344 ± 0.255, respectively) and at long-term vs. medium-term group ($P < 0.01$) (Fig. 2.C bar graph).

Table 2
Pathological findings in lung and liver tissues of BALB/c mice receiving 10 mg/kg of CEES.

Tissue/time after CEES exposure	Time-independent Observed in the short-term and continued to long term	Time-dependent Observed only in the long-term
Lung	Emphysema, atelectasis, parenchymal, inflammation/fibrosis, and congestion/hyperemia	Smooth muscle hypertrophy, goblet cells hyper/metaplasia, perivascular and per-bronchial inflammation
Liver	Granulovacuolar degeneration and necrosis	Oval cell proliferation, distribution of lobular pattern, congestion, and bile duct hyperplasia.

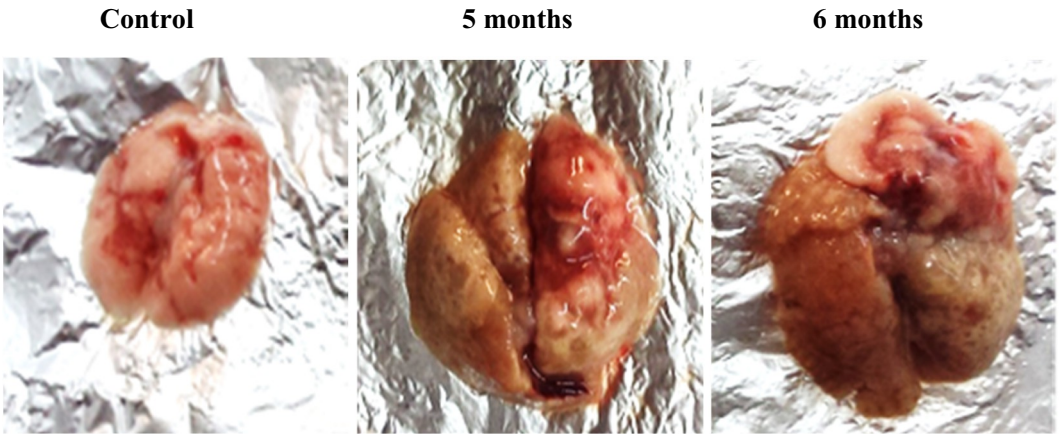

Fig. 1. The Gross view of lung tissue morphology in BALB/c mice in long-term after receiving the 10 mg/kg CEES; the severe tissue damage and increased size of lung in the CEES-receiving mouse is apparent.

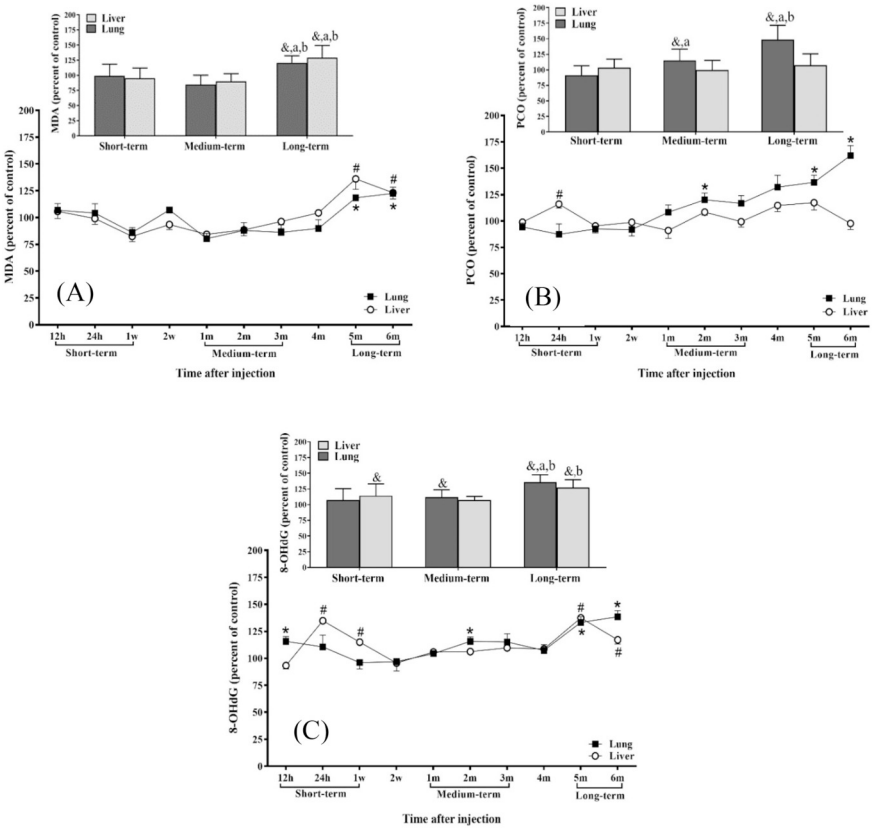

Fig. 2. MDA (A), PCO (B) and 8-OHdG (C) levels in the lung (■) and liver (○) of BALB/c mice in various time point after CEES injection. Values are expressed as a percentage of control (100%) ± S.D. In the linear graph, $^{\#}P < 0.05$ comparing test vs. control for liver and $^{*}P < 0.05$ comparing test vs. control for lung. In bar graph $^{\&}P < 0.05$ comparing test vs. control, $^{a}P < 0.05$ comparing short-term vs. other groups and $^{b}P < 0.05$ comparing long-term vs. medium-term.

3.3. The time course correlation between oxidative damage indices and percent of histopathological damage in lung and liver tissues of CEES-exposed mice

Histopathological damage of lung and liver tissues in CEES (10 mg/kg)-exposed mice were evaluated by an expert pathologist in comparison to the control. The severity of lesions was determined based on the desired pathological parameters described in Table 3 and finally expressed as the percentage of damage.

The time course correlation between oxidative damage indices and percent of histopathological damage in the lung and liver tissues of the studied mice showed a positive correlation between MDA ($r = 0.661$; $P < 0.05$), PCO ($r = 0.868$; $P < 0.01$) and 8-OHdG ($r = 0.896$; $P < 0.001$) levels and the percent of histopathological damage in the

Table 3
Desired histopathological parameters for determining the damage of lung and liver tissues.

Lung	Congestion/hyperemia, hemorrhage, perivascular inflammation, per bronchial inflammation, compensatory hyperplasia, smooth muscle hypertrophy, emphysema, atelectasis, goblet cells hyperplasia/goblet cell metaplasia, edema, parenchymal/inflammation/fibrosis
Liver	Congestion, hemorrhage, granulovacuolar degeneration, hyper/activation of Kupffer cells, fibrosis, necrosis, hepatocyte atrophy, portal hepatitis, parenchymal/hepatitis, oval cell proliferation, distribution of lobular pattern, bile duct hyperplasia

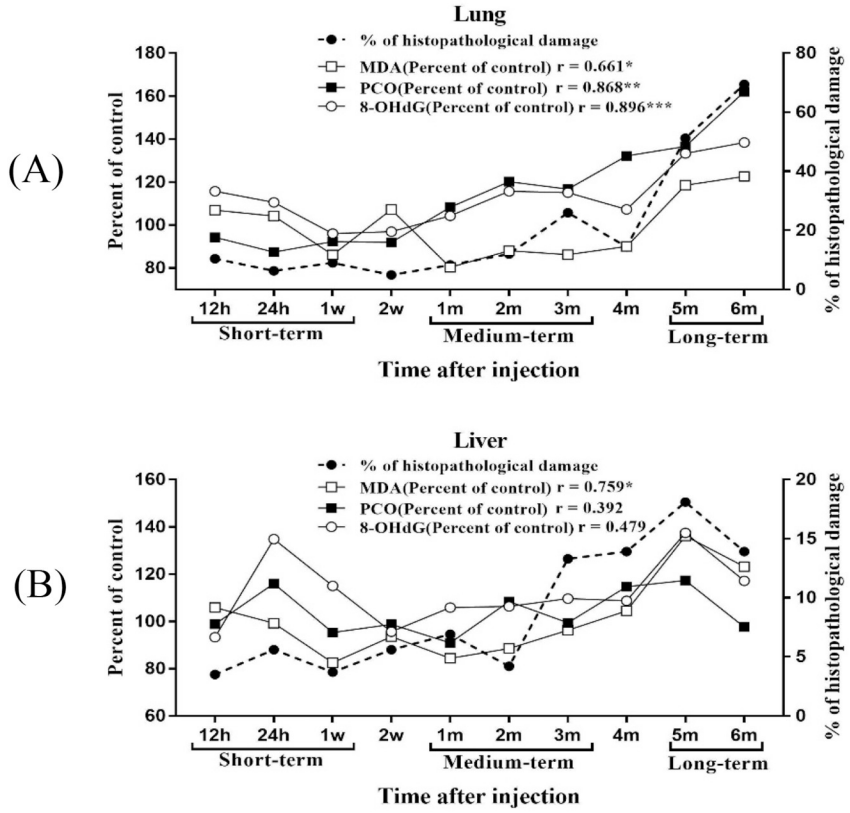

Fig. 3. Time course correlation between oxidative damage indices ((MDA (□), PCO (■) and 8-OHdG (○)) and percent of histopathological damage (●) in the lung (A) and liver (B) of BALB/c mice after CEES injection. *$P < 0.05$, **$P < 0.01$, ***$P < 0.001$.

lung tissues in CEES-exposed mice (Fig. 3.A). Moreover, a positive correlation was detected between MDA($r = 0.759$; $P < 0.05$) levels and percent of histopathological damage in liver tissue. No correlation was detected between PCO and 8-OHdG levels and the percent of histopathological damage in the liver tissues (Fig. 3.B).

3.4. The time course alteration of TOS, TAC, and OSI levels in lung and liver tissues of CEES-exposed mice

Lung TOS level (μM/gwt) was significantly increased within 12 h (1.329 ± 0.247, $P < 0.01$), 4 (1.486 ± 0.256, $P < 0.05$), 5 (1.867 ± 0.196, $P < 0.01$) and 6 (1.750 ± 0.248, $P < 0.05$) months compared to their respective control groups (0.883 ± 0.146., 1.161 ± 0.076, 1.374 ± 0.331, 1.336 ± 0.263, respectively), but in the liver, no significant change was observed at any time point (Fig. 4.A linear graph, Table 4). A significant increase was detectable in lung TOS level in long-term (1.813 ± 0.220, $P < 0.001$) vs. control (1.355 ± 0.283) and medium-term groups ($P < 0.001$). While no significant change was observed in any of the experimental groups in the liver (Fig. 4.A bar graph). TAC level in the lung and liver did not significant change at any time point in the experimental groups (Fig. 4.B, Table 4).

Lung OSI index was significantly increased within 12 h (7.77 ± 1.45, $P < 0.01$), 4 (8.1 ± 0.96, $P < 0.05$), 5 (9.1 ± 1.09, $P < 0.01$) and 6 (9.53 ± 1.24, $P < 0.05$) months in comparison with their respective control groups (5.28 ± 0.23, 6.96 ± 0.53, 6.56 ± 1.1, and 7.12 ± 1.81 respectively), but a significant change was not observed in the liver at any time point (Fig. 4.C linear graph, Table 4). The significant increase of OSI was observed in the lung within short (7.24 ± 1.24, $P < 0.05$) and long-term (9.32 ± 1.13, $P < 0.001$) vs. control groups (6.19 ± 1.01 and 6.84 ± 1.44 respectively) also long-term vs. medium-term groups ($P < 0.001$). While no significant change was observed in any of the experimental groups in the liver (Fig. 4.C bar graph).

3.5. Time-dependent change of GSSG, GSH, and GRR% levels in lung and liver tissues of CEES-exposed mice

GSSG levels (μM/g wet tissue) in the lung were decreased significantly in most groups within 24 h (0.19 ± 0.03, $P < 0.01$), 1 (0.12 ± 0.04, $P < 0.05$), 2 (0.13 ± 0.03, $P < 0.01$) weeks, and 1 months (0.13 ± 0.04, $P < 0.05$); but it was significantly increased in groups of 5 (0.18 ± 0.02, $P < 0.05$) and 6 (0.18 ± 0.01, $P < 0.001$) months compared with their respective control groups (0.27 ± 0.04, 0.19 ± 0.03, 0.19 ± 0.01, 0.18 ± 0.01, 0.14 ± 0.04, 0.12 ± 0.03, respectively). Similarly, in the liver, there was a significant decrease in the 12 (0.32 ± 0.06, $P < 0.05$) and 24 (0.48 ± 0.03, $P < 0.01$) hours and 1 month groups (0.30 ± 0.08, $P < 0.05$); but it was significantly increased in the group of 6 months (0.52 ± 0.04, $P < 0.01$) in compared to their respective control groups (0.46 ± 0.10, 0.58 ± 0.06, 0.42 ± 0.08, 0.43 ± 0.02, respectively) (Fig. 5.A. linear graph, Table 4). In both tissues, a significant decrease in GSSG level was observed in short (lung 0.15 ± 0.04, $P < 0.01$ and liver 0.42 ± 0.12, $P < 0.01$) and medium-term groups (lung 0.13 ± 0.04, $P < 0.01$ and liver 0.34 ± 0.08, $P < 0.01$), while GSSG level in long-term period (lung 0.18 ± 0.01, $P < 0.001$ and liver 0.51 ± 0.05, $P < 0.001$) was increased significantly compared to their respective control groups (lung 0.21 ± 0.06, 0.16 ± 0.03, 0.13 ± 0.04, and liver 0.53 ± 0.11, 0.43 ± 0.07, 0.42 ± 0.06, respectively), short ($P < 0.0001$) and medium-term groups ($P < 0.0001$) (Fig. 5.A. bar graph).

GSH levels (μM/g wet tissue) of the lung within 12, 24 h (0.53 ± 0.07, 0.61 ± 0.10, $P < 0.05$), 5 (0.76 ± 0.11, $P < 0.05$) and 6 (0.68 ± 0.15, $P < 0.01$) months also in the liver within 12 h (2.64 ± 0.48, $P < 0.01$), 1 (4.61 ± 0.2, $P < 0.001$), 5 (3.62 ± 0.75, $P < 0.01$) and 6 (3.19 ± 0.6, $P < 0.05$) months were

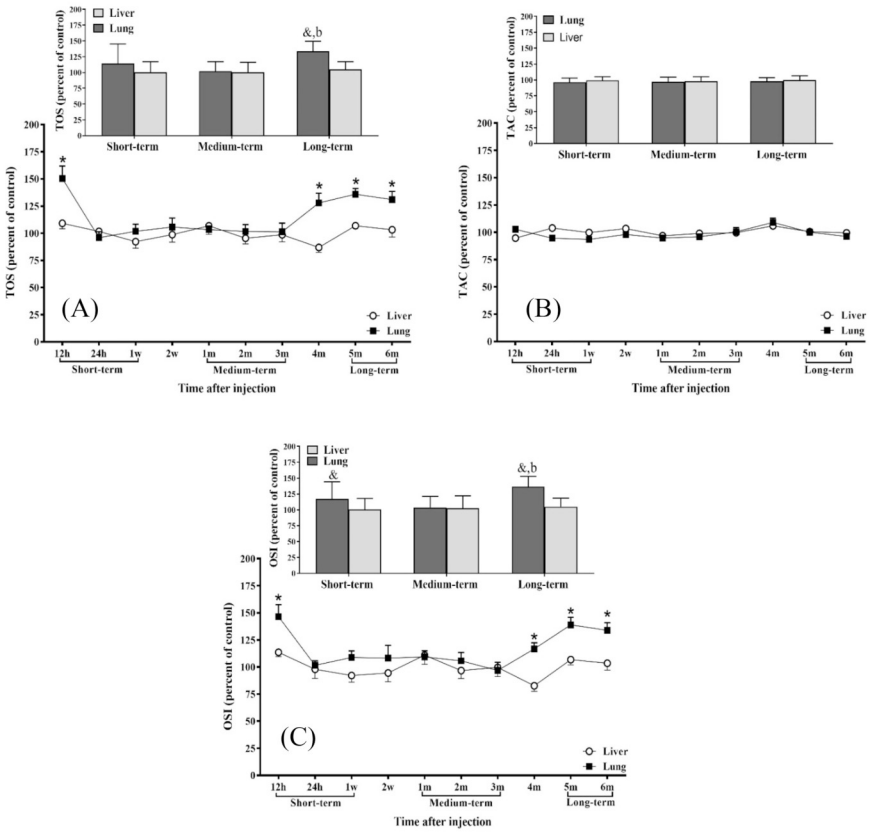

Fig. 4. TOS (A), TAC (B) and OSI (C) levels in lung (■) and liver (○) of BALB/c mice in various time point after CEES injection. Values are expressed as percentage of control (100%) ± S.D. In linear graph, $^{\#}P < 0.05$ comparing test vs. control for liver and $^{*}P < 0.05$ comparing test vs. control for lung. In bar graph $^{\&}P < 0.05$ comparing test vs. control, $^{a}P < 0.05$ comparing short-term vs. other groups and $^{b}P < 0.05$ comparing long-term vs. medium-term.

Table 4
Dynamic effect of CEES (10 mg/kg) on the oxidative stress indices and enzymatic antioxidants in the lung and liver tissues of CEES-exposed mice.

Indices		Tissue	Time after injection									
			Short-term			Medium-term				Long-term		
			12 h	24 h	1w	2w	1 m	2 m	3 m	4 m	5 m	6 m
Oxidative Stress Indices	MDA	Lung	—	—	—	—	—	—	—	—	↑	↑
		Liver	—	—	—	—	—	—	—	—	↑	↑
	PCO	Lung	—	—	—	—	—	↑	—	—	↑↑	↑↑↑
		Liver	—	↑↑	—	—	—	—	—	—	—	—
	8-OHdG	Lung	↑	—	—	—	—	↑	—	—	↑↑	↑↑
		Liver	—	↑↑↑	↑	—	—	—	—	—	↑↑↑	↑↑
	TOS	Lung	↑↑	—	—	—	—	—	—	↑	↑↑	↑
		Liver	—	—	—	—	—	—	—	—	—	—
	TAC	Lung	—	—	—	—	—	—	—	—	—	—
		Liver	—	—	—	—	—	—	—	—	—	—
	OSI	Lung	↑↑	—	—	—	—	—	—	↑	↑↑	↑
		Liver	—	—	—	—	—	—	—	—	—	—
	GSH	Lung	↓	↓	—	—	—	—	—	—	↓	↓↓
		Liver	↓↓	—	—	—	↓↓↓	—	—	—	↓↓	↓
	GSSG	Lung	—	↓↓	↓	↓↓	↓	—	—	—	↑	↑↑↑
		Liver	↓	↓↓	—	—	↓	—	—	—	—	↑↑
	GRR%	Lung	—	—	—	↓↓	↓	—	—	—	↑↑	↑↑↑
		Liver	—	—	—	—	—	—	—	—	↑	↑↑
Enzymatic Antioxidants	CAT	Lung	—	—	↓	—	—	—	—	—	—	↓↓↓↓
		Liver	—	↓↓↓	—	—	—	—	—	—	↓	↓↓
	SOD	Lung	—	—	—	—	—	—	—	—	—	↓
		Liver	—	—	—	—	—	—	—	—	—	—
	GST	Lung	—	—	↓↓	↓	↓	—	—	—	↓	↓↓↓
		Liver	—	—	—	—	—	—	—	—	—	↓↓↓↓
	GPX	Lung	—	—	—	—	—	—	—	—	—	↓
		Liver	↓↓	—	↓	—	—	—	—	—	—	↓↓
	GR	Lung	—	—	—	—	—	—	—	—	↓	↓↓
		Liver	↓↓	—	—	—	—	—	—	—	—	↓

$^{*}P < 0.05$, $^{**}P < 0.01$, $^{***}P < 0.001$ vs. control were shown by (↑), (↑↑) and (↑↑↑) respectively. In addition, (↑), (↓), and (—), respectively show an increase, decrease, and non-difference.

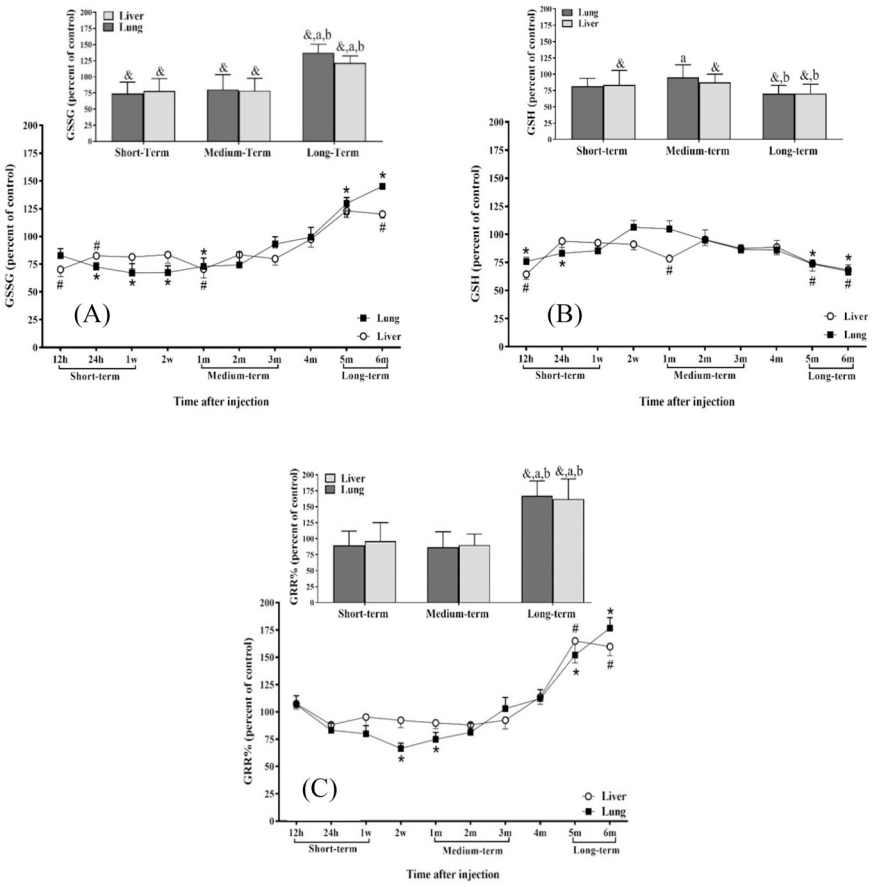

Fig. 5. GSSG (A), GSH (B) and GRR% (C) levels in the lung (■) and liver (○) of BALB/c mice in various time point after CEES injection. Values are expressed as a percentage of control (100%) ± S.D. In the linear graph, $^{\#}P < 0.05$ comparing test vs. control for liver and $^{*}P < 0.05$ comparing test vs. control for lung. In bar graph $^{\&}P < 0.05$ comparing test vs. control, $^{a}P < 0.05$ comparing short-term vs. other groups and $^{b}P < 0.05$ comparing long-term vs. medium-term.

significantly decreased compared to their respective control groups (lung 0.7 ± 0.17, 0.73 ± 0.08, 1.03 ± 0.21, 1.01 ± 0.20, and liver 4.10 ± 0.69, 5.88 ± 0.51, 4.89 ± 0.3, 4.67 ± 1.15, respectively) (Fig. 5.B. linear graph, Table 4). A significant decrease was observed in the liver GSH level in all three experimental groups (short 3.6 ± 1.03 $P < 0.05$, medium 4.44 ± 0.52 $P < 0.01$, long 3.37 ± 0.68 $P < 0.001$ respectively) compared with the control groups (short 4.269 ± 0.5, medium 5.15 ± 0.74, long 4.78 ± 0.8, respectively) also in the lung in the long-term group (0.72 ± 0.13, $P < 0.001$) compared to the control group (1.02 ± 0.19). There was a significant decrease in both tissues of long-term vs. medium-term groups (lung $P < 0.0001$ and liver $P < 0.05$) and similarly in short-term vs. medium-term groups ($P < 0.05$) in the lung only (Fig. 5.B. bar graph).

GRR% in the lung had a decreasing trend in the initial time point, significantly in groups of 2 weeks (10.37 ± 1.87 $P < 0.01$) and 1 month (11.07 ± 2.56 $P < 0.05$); but it was significantly increased in groups of 5 (18.33 ± 0.82 $P < 0.01$) and 6 (21.56 ± 4.50 $P < 0.001$) months compared with their respective control groups (15.58 ± 2.06, 14.78 ± 0.90, 12.05 ± 3.74, 10.90 ± 1.95, respectively). Similarly, GRR% in the liver was slightly decreased in most groups, but a significant increase was seen in the groups of 5 (12.37 ± 3.37 $P < 0.05$) and 6 (14.30 ± 1.97 $P < 0.01$) months compared to the control groups (7.50 ± 1.30, 8.95 ± 2.44, respectively) (Fig. 5.C. linear graph, Table 4). A significant increase of GRR% in both tissues was noticed in the long-term period (lung 20.46 ± 3.79 $P < 0.0001$ and liver 13.50 ± 2.69 $P < 0.0001$) compared to the control, (lung 11.47 ± 2.87 and liver 8.23 ± 1.35), short (lung and liver $P < 0.0001$) and medium-term groups (lung and liver $P < 0.0001$) (Fig. 5.C. bar graph).

3.6. The time course change of antioxidant enzymes including CAT, SOD, GST, GPX and GR activities in liver and lung tissues of CEES-exposed mice

CAT activity (U/mg protein) in the lung was significantly depleted within 1 week (30.60 ± 5.06, $P < 0.05$) and 6 months (16.71 ± 3.02, $P < 0.0001$) as well as in the liver within 24 h (121.4 ± 12.77, $P < 0.001$), 5 (192.74 ± 34.46, $P < 0.05$) and 6 months (109.30 ± 14.64, $P < 0.01$) compared to their respective control groups (lung 36.29 ± 1.67, 31.42 ± 2.31 and liver 168.88 ± 2.24, 232.24 ± 19.49, 174.60 ± 38.1, respectively) (Fig. 6.A. linear graph, Table 4). A significant decrease of CAT activity was detectable in both tissues in the long-term period (lung 23.76 ± 8.17 $P < 0.01$ and liver 151.02 ± 50.20 $P < 0.05$) in comparison with the control (lung 32.86 ± 4.94 and liver 203.48 ± 41.72) and medium-term groups (lung $P < 0.01$ and liver $P < 0.001$) and in long-term compared to. short-term groups ($P < 0.001$), in lung tissue only (Fig. 6.A. bar graph).

Lung and liver SOD activity (U/mg protein) did not differ significantly at any time from the study period except the 6 month group (31.79 ± 5.50, $P < 0.05$), which was significantly decreased in the lung compared to control (39.09 ± 5.64) (Fig. 6.B. linear graph, Table 4). A significant increase in the lung SOD activity was observed at within the medium-term period (58.96 ± 4.15, $P < 0.001$) in comparison with the control (53.50 ± 3.22) and short-term groups ($P < 0.001$) while there was a significant decrease in the long-term period (36.53 ± 7.06, $P < 0.05$) than control (42.77 ± 6.21), short ($P < 0.001$) and medium-term groups ($P < 0.0001$). Moreover, a significantly reduced SOD activity was detected in the liver within long-term vs. medium-term periods ($P < 0.0001$) with no significant difference in any of the three experiments groups than the control group (Fig. 6.B. bar graph).

GST activity (U/mg protein) in lung tissue within 1 (1.07 ± 0.18,

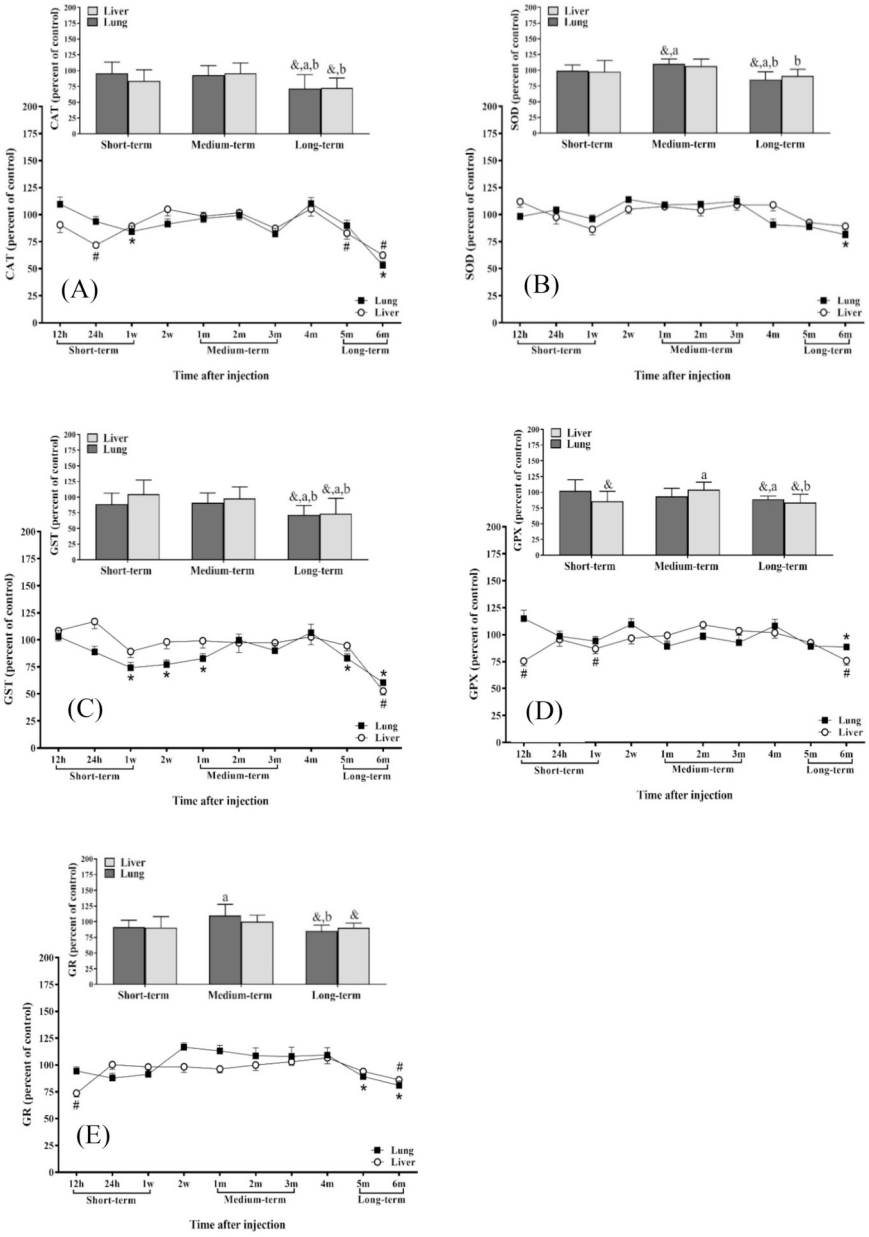

Fig. 6. Antioxidant enzymes including CAT (A), SOD (B), GST (C), GPX (D) and GR (E), activities in the lung (■) and liver (○) of BALB/c mice in various time point after CEES injection. Values are expressed as a percentage of control (100%) ± S.D. In the linear graph, $^{\#}P < 0.05$ comparing test vs. control for liver and $^{*}P < 0.05$ comparing test vs. control for lung. In bar graph $^{\&}P < 0.05$ comparing test vs. control, $^{a}P < 0.05$ comparing short-term vs. other groups and $^{b}P < 0.05$ comparing long-term vs. medium-term.

$P < 0.01$), 2 (1.09 ± 0.17, $P < 0.05$) weeks, 1 (1.24 ± 0.2, $P < 0.05$), 5 (1.16 ± 0.15, $P < 0.05$) and 6 (0.64 ± 0.1, $P < 0.001$) months was significantly lower than their respective control groups (1.44 ± 0.11, 1.38 ± 0.16, 1.5 ± 0.1, 1.38 ± 0.15, 1.04 ± 0.17, respectively), but no significant changes were observed in the liver tissue, except for a significant reduction within sixth month (9.19 ± 1.67, $P < 0.0001$) in comparison with the control (17.44 ± 2.31) (Fig. 6.C. linear graph, Table 4). A significant decrease of lung and liver GST activity was noticed within the long-term period (lung 0.9 ± 0.29, $P < 0.05$ and liver 12.89 ± 4.3, $P < 0.01$) as compared to the control (lung 1.21 ± 0.23 and liver 17.49 ± 2.27), short (lung $P < 0.01$ and liver $P < 0.001$) and medium-term groups (lung $P < 0.001$ and liver $P < 0.01$) (Fig. 6.C. bar graph).

The change in lung GPX activity (U/mg protein) was not significant at any time point from the study period except for a significant reduction within sixth month (0.61 ± 0.04, $P < 0.05$) compared to the control (0.69 ± 0.06). However, a significant decrease was observed in the liver within 12 h (2.94 ± 0.46, $P < 0.01$), 1 week (3.06 ± 0.42, $P < 0.05$) and sixth month (5.21 ± 0.78, $P < 0.01$) in comparison with their respective control groups (3.9 ± 0.41, 3.52 ± 0.17, 6.86 ± 0.85, respectively) (Fig. 6.D. linear graph, Table 4). A significant decrease was noticed in the lung GPX activity within the long-term (0.57 ± 0.05, $P < 0.05$) vs. control (0.64 ± 0.08) and short-term groups ($P < 0.01$) and similarly, within short (3.08 ± 0.48, $P < 0.01$) and long-term (6.16 ± 1.31, $P < 0.05$) vs. control groups (3.6 ± 0.4, 7.36 ± 0.91) and medium-term groups ($P < 0.001$, $P < 0.0001$) in the liver (Fig. 6.D. bar graph).

GR activity (U/mg protein) in the lung was significantly depleted within 5 (0.24 ± 0.02, $P < 0.05$) and 6 month (0.23 ± 0.03, $P < 0.01$) as well as in the liver within 12 h (0.5 ± 0.06, $P < 0.01$) and 6 months (0.68 ± 0.06, $P < 0.05$) in comparison to their respective control groups (lung 0.27 ± 0.02, 0.29 ± 0.02 and liver

0.68 ± 0.09, 0.79 ± 0.06, respectively) (Fig. 6.E. linear graph, Table 4). A significant decrease was observed in GR activity in both tissues in the long-term group (lung 0.24 ± 0.02, $P < 0.001$, and liver 0.70 ± 0.05, $P < 0.01$) compared with the control (lung 0.28 ± 0.02 and liver 0.78 ± 0.06); besides, there was a significant decrease within the long and short-term vs. medium-term groups ($P < 0.0001$, $P < 0.001$) in the lung (Fig. 6.E. bar graph).

4. Discussion

The toxicological effects of SM have been explained by several cellular and molecular mechanisms. According to some of them, oxidative stress plays an important role in the development of SM-induced injuries by massive production of ROS and depletion of antioxidant defense systems [14,15]. Human studies indicate that SM-induced disorders have worsened over time [60]. However, there are very few reports that describe the effects of SM on oxidative parameters and antioxidant system over time from short to long-term periods [61]. Time course study of these changes in response to SM is very important for a better understanding of the acute and delayed events of SM and the pathophysiological basis of SM-induced injuries. Such investigations could lead to new therapeutic approaches preventing disease progression.

In the present study, the animals were exposed to CEES by intraperitoneal route for developing the systemic contamination. Then, we performed a time-course analysis (short, medium, and long-term) of the oxidative stress biomarkers and cellular antioxidant systems in the lung and liver tissues of CEES-exposed mice. These tissues have various structures, composition, and functions. In addition, the lung was considered as an organ with the most delayed disorder induced by SM (respiratory problems are the greatest cause of long-term disability in SM-exposed veterans), and the liver as an organ that has an important role in detoxification and metabolism of xenobiotics such as SM or their metabolites. Therefore, regarding the choice of intraperitoneal route and the different antioxidant capacity of these organs, it is expected that the severity of response and alteration of the oxidant and antioxidant parameters induced by CEES in these organs will be different.

Malondialdehyde as a final product of lipid peroxidation can be used as an indicator for measuring the damage from free radical production in tissue membranes [62]. In this study, the evaluation of time course changes of MDA levels in the lung and liver tissues of CEES-exposed mice revealed insignificant increase of MDA levels in the short-term (12 and 24 h) and this insignificancy is probably due to the proper functioning of the enzymatic and non-enzymatic antioxidant system during the first hours of exposure to CEES. While, the delayed increase in MDA levels in the long-term group (5 and 6 m) can be a direct reflection of the oxidative damage in both tissues. To date, no studies have measured MDA levels in the lung tissue of patients with SM-induced lung injuries. However, a number of the previous studies have shown the elevated levels of MDA in serum, bronchoalveolar lavage fluids (BALF) and sputum of these patients in the delayed phase after SM-exposure [14,63,64].

PCO level, as the biomarker of oxidative stress, was increased in the lung tissue during the study period, especially within the medium-term (2 month) and long-term periods (5 and 6 month). These findings suggest a delayed increase in the oxidative stress status in the lung of CESS-exposed mice compared to the controls. While, except for 24 h, no significant change was found at any time point of the study period in the liver tissue. It is probably due to the high antioxidant capacity and detoxification activity of the liver tissue compared to the lung tissue [65]. In this regard, Tahmasbpour Marzony has reported an increased level of PCO in the BAL fluid of SM-exposed patient [64].

8-OHdG (DNA oxidative damage marker) revealed an initial increase (12h) in the lung tissue. This increase was more significant especially in the long-term (5 and 6 m) groups compared to the control. The same trend was also observed in the liver tissue with a slight difference, so that 8-OHdG had shown a higher increase in liver (24 h and 1 week) than lung, which is in line with intraperitoneal administration route. This data indicated that DNA repair mechanisms do not respond to the damage caused by CEES. Therefore, DNA damage is an early and late event after CEES exposure. Similarity, O'neill et al. reported that 8-OHdG level increases at 18 h after CEES inhalation in rats [66].

Evaluation of time course correlation between oxidative damage indices and percent of histopathological damage indicated that there is a positive correlation between MDA, PCO, and 8-OHdG levels and the percent of histopathological damage in the lung tissues; moreover, a positive correlation was detected between MDA levels and percent of histopathological damage in liver tissue. This correlation finding confirms and supports the fact that time course production of ROS and oxidative injury play an important role in the development of SM-induced injuries.

TAC and TOS provide the feasibility of evaluating all the oxidant and antioxidant molecules together. OSI (TOS/TAC) is an index of the oxidative stress degree and indicates the oxidant/antioxidant redox balance [67]. Our results showed that in the lung tissue, TOS and OSI were significantly increased within 12 h and then in the long-term periods from 4 to 6 months compared to the control group. Although a similar pattern of lung changes was observed in the liver tissue, it was not significant at any studied time points. The observed difference in TOS and OSI between lung and liver tissues is probably due to the high antioxidant capacity and detoxification activity of the liver than the lung tissue [65]. The TAC levels showed no significant difference between the control and test group in both tissues. The data indicated that oxidative stress, as a biomarker in the lung, is a short and long-term event after CEES exposure. To the best of our knowledge, few studies have examined TAC and TOS in animal models or SM-exposed patients. Marzony et al. observed the declined levels of TAC in BAL fluids of SM-exposed patients [68]. In addition, an increase in TOS levels was reported by Soroush et al. in SM-exposed veterans [69].

GSH is an important non-enzymatic antioxidant that plays a crucial role in both scavenging oxyradicals and detoxification of reactive chemicals. GSH serves as a cofactor or hydrogen donor for several antioxidant enzymes including GST and GPX [63,70]. The results showed that the GSH levels of lung and liver tissues of CEES-exposed mice were significantly decreased in the short-term perid and subsequently recovered to normal in the medium-term period and once again decreased in the long-term period. Depletion of GSH may be due to (1) the loss of GSH through CEES complex formation followed by metabolism and/or excretion, (2) increased use of GSH in protecting SH-containing proteins from ROS, (3) decline in the expression (low expression or down-regulation) of enzymes involved in GSH production. This depletion can reduce the productivity of antioxidant enzymes (GST and GPX) and enhance ROS and oxidative injury [71,72]. GSH prevents the oxidation of proteins in the cell cytoplasm, and probably, the observed reduction of GSH leads to an increase of PCO levels in the lung tissue within the long-term period. However, the decrease of liver GSH is not associated with an increase in PCO levels in the long-term period, because of the faster turnover of GSH in the liver than the lung [65]. There are many similar reports in short-term animal models and long-term human studies that are in accordance with our data [61,73,74]. In addition, depletion of GSH frequently was reported in serum, BAL fluids, and sputum of patients several years after SM exposure [14,25,63,75]. Several clinical trial studies have indicated that treatment with GSH precursors in SM-exposed patients with delayed lung injury can decrease markers of oxidative stress and SM-toxicity [30,76,77]. These findings highlight the importance of cellular GSH as a defense mechanism against oxidative stress and lung damages.

Concomitant with GSH changes, the GSSG levels of lung and liver tissues in the short and medium-term periods were significantly decreased in most time groups, while in the long-term period, a significant increase was observed in 5 and 6 month groups.

GRR%, as an index of oxidative stress, showed a decreasing trend in the short and medium-term periods in both tissues and then significantly increased in the long-term periods compared to the control group. These findings suggest that an oxidative-antioxidant imbalance may be considered as one of the major disorders in CEES-induced delayed damage. The outcome of such an imbalance is consistent with the finding of SM-exposure individual indicating that their injuries are getting worse over time.

The current study results showed that the activity of enzymatic antioxidants including CAT, SOD, GST, GPX, and GR in the lung and liver tissues of CEES-exposed mice changed almost with the same pattern; they were first decreased in the short-term period, then reached the normal level in the medium-term period, and significantly decreased during the long-term period.

SOD and CAT are the most important enzymatic antioxidants against oxidative stress. SOD catalyzes the conversion of radical superoxide to hydrogen peroxide (H_2O_2), and CAT protects cells against the toxic effects of H_2O_2 by decomposing it into oxygen and water [78,79]. Our results in short-term periods are consistent with the study by Jafari that showed the intraperitoneal application of acute SM doses (> 10 mg/kg) decreased SOD and CAT activities in liver and brain of the rat within 2 and 7 days post-treatment [61]. In addition, Husain et al. showed that 24 h after percutaneous application of SM (0.5 LD50), the activity of SOD and CAT in blood cells and body tissues of rats were reduced [80]. Regarding our long-term results, there are numerous reports of reduced activity of these enzymes in the long-term period after exposure to SM [26,81–83]. Mirbagheri et al. reported up-regulation and down-expression of SOD mRNA and SOD proteins respectively in the lung of SM-exposed patients [81]. Similar findings revealed a significant reduction of SOD and CAT activity in the serum of these patients [82]. It worth noting that, the approximate stability of SOD activity in the liver is consistent with the trend of TOS changes in this tissue.

GST, as a supporting antioxidant enzyme, was proposed to play an important role in cellular detoxification of xenobiotics and endobiotics by conjugation with GSH, thereby by neutralizing and increasing their dissolution, leads to their excretion from cells [56]. On the other hand, some of the GST isoforms protect cells against oxidative stress products by breaking peroxidation chain reactions through the removal of hydrogen peroxide, and ultimately with both its functions limit tissue damage [29]. The relative levels of GSH and GST activities in the liver and lung may be an important factor in the relative susceptibility of these organs to the toxic effects of xenobiotics. It has been reported that the GSTs activity is considerably lower in the lung than the liver under normal conditions. Therefore, the conjugation of xenobiotics and their metabolites with GSH might be notably slower in the lung [23,65]. Obtained results in our study showed that the intensity of GST changes over time in the lung was higher than the liver. In addition, our findings are consistent with previous works reporting the reduction of GST after SM exposure. A decrease of GST activity within 8 and 24 h in the skin of mice treated with 2 mg of CEES was reported by Kim et al. [84]. Nourani et al. reported the overexpression of GST mRNA in the lung biopsies of SM-exposed patients, while immunohistochemistry analysis for GSTs expression in protein levels was negative compared to the control [85]. Using multiplex PCR method, Dastjerdi et al. showed the frequency of GSTM1 homozygous deletion was significantly higher in SM-exposed patients at severe/very severe stage of lung complications compared to the subjects with mild/moderate lung complications [86].

GPX is an intracellular selenocysteine-containing enzyme acting as a catalyzer to reduce lipid and hydrogen peroxides to their corresponding alcohols, thereby protecting the body against oxidative stress. In addition, GPX uses GSH as an obligate co-substrate in the reduction of hydrogen peroxide to water to limit the harmful effects of hydroxyl peroxides [87]. Several investigations have shown a reduction of GPX activity in SM-exposed rats in the lung, liver and serum samples, which is in agreement with our data [80,88,89].

GR, as dimeric disulfide oxidoreductase, utilizes a FAD prosthetic group and NADPH to reduce one molar equivalent of GSSG to two molar equivalents of GSH. The reaction is essential for the maintenance of glutathione levels in the reduced form [90]. Several studies have reported GR deficiency in SM-exposed patients, which is in accordance with our data [29,91].

According to Sawale et al. the level of intracellular GSH and activity of GR, GPX, and GST enzymes were decreased following the CEES-exposure [92]. Thus, GSH contents and the activity of these antioxidants in oxidatively damaged cells are strongly correlated. The reduction of GSH in the acute phase may be related to GSH binding to SM toward metabolizing and excreting SM from the body. In the delayed phase, while there is no trace of SM, depletion of GSH frequently was reported in serum, BAL fluids, and sputum of SM-exposed patients. The actual mechanism by which SM decreases cellular GSH contents in this phase is not clear. To find a likely response, several studies have evaluated the effect of SM on the expression and activity of various antioxidant enzymes at the delayed phase of SM-injury [93]. Two of the most recent studies have revealed up-regulation of GST, and GPX mRNAs in mustard lung biopsies of SM-injured patients, while GR was significantly down regulated [25,93]. Nevertheless, the expression of these antioxidants at the protein levels was not investigated. Given that our results in the lung and liver tissues show a significant decrease in GR activity in the long-term phase, it is expected that the decline in GR activity to be related to the reduction of protein expression levels. Note that upregulated genes do not essentially translated into higher protein expression levels. Therefore, the reduced activity of GPX and GST observed in the long-term phase of the current study may be related to the deficiencies in GR and the regeneration of GSH, because depletion of GSH as a cofactor for GST and GPX may decline the activity and productivity of these enzymes in cells. In the absence of these enzymes, the antioxidant defense is decreased leading to the increased ROS accumulation and oxidative injury [25,94]. These events can ultimately result in inflammation and accumulation of neutrophils, and the generation of more ROS and more severe damage associated with cell death and necrosis of the tissue, which are confirmed by our histopathological outcome.

In conclusion, obtained results showed an increase in oxidative damage markers and a reduction in the antioxidant defense system in both lung and liver tissues in the short-term period, while these variables return to normal in the medium-term period. In addition, in the long-term, we observed a significant increase in oxidative damage markers and a significant reduction in the antioxidant defense system once more. This reduction is considered as a mechanism by which CEES can enhance ROS accumulation and oxidative injury. It can be supported by the determined positive correlation between oxidative damage indices (increased levels of MDA, PCO, and 8OH-dG) and the percent of histopathological damage. In addition the efficacy of other routes for CEES administration should be studied over time and compared with the results of the present study.

References

[1] M. Valko, D. Leibfritz, J. Moncol, M.T.D. Cronin, M. Mazur, J. Telser, Free radicals and antioxidants in normal physiological functions and human disease, Int. J. Biochem. Cell Biol. 39 (2007) 44–84.
[2] D. Trachootham, W. Lu, M.A. Ogasawara, N.R.-D. Valle, P. Huang, Redox regulation of cell survival, Antioxid. Redox Signal. 10 (2008) 1343–1374.
[3] X. Wang, H. Fang, Z. Huang, W. Shang, T. Hou, A. Cheng, H. Cheng, Imaging ROS signaling in cells and animals, J. Mol. Med. 91 (2013) 917–927.
[4] W. Droge, Free radicals in the physiological control of cell function, Physiol. Rev. 82 (2002) 47–95.
[5] M. Nita, A. Grzybowski, The role of the reactive oxygen species and oxidative stress in the pathomechanism of the age-related ocular diseases and other pathologies of the anterior and posterior eye segments in adults, Oxidative Med. Cell. Longev. 2016 (2016).
[6] N. Bashan, J. Kovsan, I. Kachko, H. Ovadia, A. Rudich, Positive and negative regulation of insulin signaling by reactive oxygen and nitrogen species, Physiol. Rev. 89 (2009) 27–71.

[7] X. Li, P. Fang, J. Mai, E.T. Choi, H. Wang, X. Yang, Targeting mitochondrial reactive oxygen species as novel therapy for inflammatory diseases and cancers, J. Hematol. Oncol. 6 (2013) 19.

[8] G.G. Ortiz, F.P. Pacheco-Moisés, O.K. Bitzer-Quintero, A.C. Ramírez-Anguiano, L.J. Flores-Alvarado, V. Ramírez-Ramírez, M.A. Macias-Islas, E.D. Torres-Sánchez, Immunology and oxidative stress in multiple sclerosis: clinical and basic approach, Clin. Dev. Immunol. 2013 (2013).

[9] D.E. Coricovac, C.A. Dehelean, Pathological aspects with global impact induced by toxicants at cellular level, Toxicol. Stud. Drugs Environ, InTech, 2015.

[10] T. Davidson, Q. Ke, M.A.X. Costa, Selected molecular mechanisms of metal toxicity and carcinogenicity, Handb. Toxicol. Met, Fourth ed., Elsevier, 2015, pp. 173–196.

[11] K. Kehe, L. Szinicz, Medical aspects of sulphur mustard poisoning, Toxicology 214 (2005) 198–209, https://doi.org/10.1016/j.tox.2005.06.014.

[12] M.R. Naghii, Sulfur mustard intoxication, oxidative stress, and antioxidants, Mil. Med. 167 (2002) 573–575.

[13] V. Paromov, Z. Suntres, M. Smith, W.L. Stone, Sulfur mustard toxicity following dermal exposure: role of oxidative stress, and antioxidant therapy, J Burn. Wounds. 7 (2007) e7.

[14] M. Shohrati, M. Ghanei, N. Shamspour, F. Babaei, M.N. Abadi, M. Jafari, A.H. Ali, Glutathione and malondialdehyde levels in late pulmonary complications of sulfur mustard intoxication, Lung 188 (2010) 77–83.

[15] E. Tahmasbpour, S. Reza Emami, M. Ghanei, Y. Panahi, Role of oxidative stress in sulfur mustard-induced pulmonary injury and antioxidant protection, Inhal. Toxicol. 27 (2015) 659–672.

[16] S. Mansour Razavi, P. Salamati, M. Saghafinia, M. Abdollahi, A review on delayed toxic effects of sulfur mustard in Iranian veterans, Daru 20 (2012) 51, https://doi.org/10.1186/2008-2231-20-51.

[17] Z. Nokhodian, F. ZareFarashbandi, P. Shoaei, Mustard gas exposure in Iran–Iraq war–a scientometric study, J. Educ. Health Promot. 4 (2015).

[18] S. Ahmad, A. Ahmad, Emerging targets for treating sulfur mustard-induced injuries, Ann. N. Y. Acad. Sci. 1374 (2016) 123–131, https://doi.org/10.1111/nyas.13095.

[19] Y. Panahi, M. Ghanei, M.V. Zarch, Z. Poursaleh, S. Parvin, R. Rezaee, A. Sahebkar, Evaluation of the pharmacoeconomics of drugs used for the treatment of long-term complications of sulfur mustard, Ital. J. Med. 11 (2016) 102–113.

[20] M. Balali-Mood, M. Hefazi, Comparison of early and late toxic effects of sulfur mustard in Iranian veterans, Basic Clin Pharmacol Toxicol 99 (2006) 273–282, https://doi.org/10.1111/j.1742-7843.2006.pto_429.x.

[21] H. Davoodzadeh, H. Rahmani, Systemic inflammation in chemical lung veterans with mustard gas, Persian J. Med. Sci. 2 (2015).

[22] K. Ghabili, P.S. Agutter, M. Ghanei, K. Ansarin, Y. Panahi, M.M. Shoja, Sulfur mustard toxicity: history, chemistry, pharmacokinetics, and pharmacodynamics, Crit. Rev. Toxicol. 41 (2011) 384–403, https://doi.org/10.3109/10408444.2010.541224.

[23] Y. Panahi, M. Ghanei, A. Hajhashemi, A. Sahebkar, Effects of curcuminoids-piperine combination on systemic oxidative stress, clinical symptoms and quality of life in subjects with chronic pulmonary complications due to sulfur mustard: a randomized controlled trial, J Diet Suppl 13 (2016) 93–105, https://doi.org/10.3109/19390211.2014.952865.

[24] B. Weinberger, J.D. Laskin, V.R. Sunil, P.J. Sinko, D.E. Heck, D.L. Laskin, Sulfur mustard-induced pulmonary injury: therapeutic approaches to mitigating toxicity, Pulm. Pharmacol. Ther. 24 (2011) 92–99.

[25] I. Layali, A. Shahriary, N. Rahmani Talatappe, E. Tahmasbpour, H. Rostami, A. Beigi Harchegani, Sulfur mustard triggers oxidative stress through glutathione depletion and altered expression of glutathione-related enzymes in human airways, Immunopharmacol. Immunotoxicol. (2018) 1–7.

[26] A. Beigi Harchegani, E. Tahmasbpour, H. Borna, A. Imamy, M. Ghanei, A. Shahriary, Free radical production and oxidative stress in lung tissue of patients exposed to sulfur mustard: an overview of cellular and molecular mechanisms, Chem. Res. Toxicol. 31 (2018) 211–222.

[27] K. Ghabili, P.S. Agutter, M. Ghanei, K. Ansarin, M.M. Shoja, Mustard gas toxicity: the acute and chronic pathological effects, J. Appl. Toxicol. 30 (2010) 627–643.

[28] M. Ghanei, A.A. Harandi, Molecular and cellular mechanism of lung injuries due to exposure to sulfur mustard: a review, Inhal. Toxicol. 23 (2011) 363–371.

[29] J.D. Laskin, A.T. Black, Y. Jan, P.J. Sinko, N.D. Heindel, V. Sunil, D.E. Heck, D.L. Laskin, Oxidants and antioxidants in sulfur mustard–induced injury, Ann. N. Y. Acad. Sci. 1203 (2010) 92–100.

[30] M. Shohrati, I. Karimzadeh, A. Saburi, H. Khalili, M. Ghanei, The role of N-acetylcysteine in the management of acute and chronic pulmonary complications of sulfur mustard: a literature review, Inhal. Toxicol. 26 (2014) 507–523.

[31] A. Emad, Y. Emad, Levels of cytokine in bronchoalveolar lavage (BAL) fluid in patients with pulmonary fibrosis due to sulfur mustard gas inhalation, J. Interf. Cytokine Res. 27 (2007) 38–43.

[32] M.R. Keramati, M. Balali-Mood, S.R. Mousavi, M. Sadeghi, B. Riahi-Zanjani, Biochemical and hematological findings of Khorasan veterans 23 years after sulfur mustard exposure, J. Res. Med. Sci. Off. J. Isfahan Univ. Med. Sci. 18 (2013) 855.

[33] A. Taravati, S.K. Ardestani, M.-R. Soroush, S. Faghihzadeh, T. Ghazanfari, F. Jalilvand, M.M. Naghizadeh, F. Fallahi, Serum albumin and paraoxonase activity in Iranian veterans 20 years after sulfur mustard exposure, Immunopharmacol. Immunotoxicol. 34 (2012) 706–713.

[34] S.J. Biswas, S. Pathak, A.R. Khuda-Bukhsh, Assessment of the genotoxic and cytotoxic potential of an anti-epileptic drug, phenobarbital, in mice: a time course study, Mutat. Res. Toxicol. Environ. Mutagen. 563 (2004) 1–11.

[35] J. Fernandes, K. Uppal, K.H. Liu, X. Hu, Y.-M. Go, D. Jones, Time-course metabolomic analysis of manganese toxicity reveals biomarkers of oxidative stress and amino acid metabolism as early cellular targets, Free Radic. Biol. Med. 128 (2018) S83.

[36] M.J. Marks, J.A. Stitzel, A.C. Collins, Time course study of the effects of chronic nicotine infusion on drug response and brain receptors, J. Pharmacol. Exp. Ther. 235 (1985) 619–628.

[37] J. Pedraza-Chaverrí, D. Barrera, O.N. Medina-Campos, R.C. Carvajal, R. Hernández-Pando, N.A. Macías-Ruvalcaba, P.D. Maldonado, M.I. Salcedo, E. Tapia, L. Saldívar, Time course study of oxidative and nitrosative stress and antioxidant enzymes in K2Cr2O7-induced nephrotoxicity, BMC Nephrol. 6 (2005) 4.

[38] F.J. Salguero, W.L. Garcia-Jimenez, I. Lima, K. Seifert, Histopathological and immunohistochemical characterisation of hepatic granulomas in Leishmania donovani-infected BALB/c mice: a time-course study, Parasit. Vectors 11 (2018) 73.

[39] S.K. Das, S. Mukherjee, M.G. Smith, D. Chatterjee, Prophylactic protection by N-acetylcysteine against the pulmonary injury induced by 2-chloroethyl ethyl sulfide, a mustard analogue, J. Biochem. Mol. Toxicol. 17 (2003) 177–184.

[40] S.D. McClintock, L.M. Hoesel, S.K. Das, G.O. Till, T. Neff, R.G. Kunkel, M.G. Smith, P.A. Ward, Attenuation of half sulfur mustard gas-induced acute lung injury in rats, J. Appl. Toxicol. An Int. J. 26 (2006) 126–131.

[41] T. Ghazanfari, S. Kaboudanian Ardestani, M. Varmazyar, M. Eghtedar Doost, F. Heidari, Z. Kianmehr, R. Gharebaghi, R. Sedaghat, H. Ghasemi, M.M. Naghizadeh, M. Heshmati, M.R. Vaez-Mahdavi, S. Faghihzadeh, A mouse model of acute and delayed complications of sulfur mustard analogue, 2-chloroethyl ethyl sulfide, Immunoregulation 1 (2018) 127–142, https://doi.org/10.32598/IMMUNOREGULATION.1.3.127.

[42] S.C. Gad, C.S. Weil, Statistics for toxicologists, Princ. Methods Toxicol. 2 (1982) 273–320.

[43] N. Geifman, E. Rubin, The mouse age phenome knowledgebase and disease-specific inter-species age mapping, PLoS One 8 (2013) e81114.

[44] H. Ohkawa, N. Ohishi, K. Yagi, Assay for lipid peroxides in animal tissues by thiobarbituric acid reaction, Anal. Biochem. 95 (1979) 351–358.

[45] R.L. Levine, D. Garland, C.N. Oliver, A. Amici, I. Climent, A.-G. Lenz, B.-W. Ahn, S. Shaltiel, E.R. Stadtman, Determination of carbonyl content in oxidatively modified proteins, Methods Enzymol, Elsevier, 1990, pp. 464–478.

[46] A.Z. Reznick, Lester Packer, Oxidative damage to proteins: spectrophotometric method for carbonyl assay, Method Enzymol 233 (1994) 357–363, https://doi.org/10.1016/S0076-6879(94)33041-7.

[47] M. Hermes-Lima, W.G. Willmore, K.B. Storey, Quantification of lipid peroxidation in tissue extracts based on Fe (III) xylenol orange complex formation, free radic, Biol. Med. 19 (1995) 271–280.

[48] O. Erel, A new automated colorimetric method for measuring total oxidant status, Clin. Biochem. 38 (2005) 1103–1111.

[49] R. Re, N. Pellegrini, A. Proteggente, A. Pannala, M. Yang, C. Rice-Evans, Antioxidant activity applying an improved ABTS radical cation decolorization assay, Free Radic. Biol. Med. 26 (1999) 1231–1237.

[50] M. Rabus, R. Demirbağ, Y. Sezen, O. Konukoğlu, A. Yildiz, O. Erel, R. Zeybek, C. Yakut, Plasma and tissue oxidative stress index in patients with rheumatic and degenerative heart valve disease, Turk Kardiyol Dern Ars 36 (2008) 536–540.

[51] O.W. Griffith, Determination of glutathione and glutathione disulfide using glutathione reductase and 2-vinylpyridine, Anal. Biochem. 106 (1980) 207–212.

[52] F. Tietze, Enzymic method for quantitative determination of nanogram amounts of total and oxidized glutathione: applications to mammalian blood and other tissues, Anal. Biochem. 27 (1969) 502–522.

[53] I. Németh, D. Boda, Blood glutathione redox ratio as a parameter of oxidative stress in premature infants with IRDS, Free Radic. Biol. Med. 16 (1994) 347–353.

[54] H. Aebi, [13] Catalase in vitro, in: Methods Enzymol., Elsevier, 1984: pp. 121–126.

[55] A.V. Peskin, C.C. Winterbourn, A microtiter plate assay for superoxide dismutase using a water-soluble tetrazolium salt (WST-1), Clin. Chim. Acta 293 (2000) 157–166.

[56] W.H. Habig, M.J. Pabst, W.B. Jakoby, Glutathione S-transferases the first enzymatic step in mercapturic acid formation, J. Biol. Chem. 249 (1974) 7130–7139.

[57] L. Flohé, W.A. Günzler, [12] assays of glutathione peroxidase, Methods Enzymol, Elsevier, 1984, pp. 114–120.

[58] A.E. Cribb, J.S. Leeder, S.P. Spielberg, Use of a microplate reader in an assay of glutathione reductase using 5,5′-dithiobis (2-nitrobenzoic acid), Anal. Biochem. 183 (1989) 195–196.

[59] M.M. Bradford, A rapid and sensitive method for the quantitation of microgram quantities of protein utilizing the principle of protein-dye binding, Anal. Biochem. 72 (1976) 248–254.

[60] M. Balali-Mood, M. Hefazi, The pharmacology, toxicology, and medical treatment of sulphur mustard poisoning, Fundam. Clin. Pharmacol. 19 (2005) 297–315.

[61] M. Jafari, Dose-and time-dependent effects of sulfur mustard on antioxidant system in liver and brain of rat, Toxicology 231 (2007) 30–39.

[62] D. Ritter, J.W. Knebel, M. Aufderheide, U. Mohr, Development of a cell culture model system for routine testing of substances inducing oxidative stress, Toxicol. Vitr. 13 (1999) 745–751.

[63] J. Heydari, M. Jafari, S. Khazaie, H. Goosheh, M. Ghanei, A. Karbasi, The role of oxidative stress in severity of obstructive pulmonary complications in sputum of sulfur mustard-injured patients, Iran. J. Toxicol. 11 (2017) 5–11.

[64] E. Tahmasbpour Marzony, M. Ghanei, Y. Panahi, Oxidative stress and altered expression of peroxiredoxin genes family (PRDXS) and sulfiredoxin-1 (SRXN1) in human lung tissue following exposure to sulfur mustard, Exp. Lung Res. 42 (2016) 217–226.

[65] M.S. Moron, J.W. Depierre, B. Mannervik, Levels of glutathione, glutathione reductase and glutathione S-transferase activities in rat lung and liver, Biochim. Biophys. Acta - Gen. Subj. 582 (1979) 67–78, https://doi.org/10.1016/0304-4165(79)90289-7.

[66] H.C. O'neill, C.W. White, L.A. Veress, T.B. Hendry-Hofer, J.E. Loader, E. Min, J. Huang, R.C. Rancourt, B.J. Day, Treatment with the catalytic metalloporphyrin

AEOL 10150 reduces inflammation and oxidative stress due to inhalation of the sulfur mustard analog 2-chloroethyl ethyl sulfide, Free Radic. Biol. Med. 48 (2010) 1188–1196.
[67] O. Erel, A novel automated method to measure total antioxidant response against potent free radical reactions, Clin. Biochem. 37 (2004) 112–119.
[68] E.T. Marzony, A. Nejad-Moghadam, M. Ghanei, Y. Panahi, Sulfur mustard causes oxidants/antioxidants imbalance through the overexpression of free radical producing-related genes in human mustard lungs, Environ. Toxicol. Pharmacol. 45 (2016) 187–192.
[69] M.P.H. Soroush M.R.1 MD Faday Vatan R.* MD, MPH, PhD, Sahaf R.2 MD, MHSc, PhD, Taravati A.3 PhD, F.S. P. Ghazanfari T.4 PhD Kaboudiyan Ardestani S.6 PhD, Correlation of oxidative stress indices with age in chemical veterans with severe pulmonary complication; longtime after exposition to sulfur mustard, Iran. J. War Public Heal. 6 (2014) 183–187.
[70] A. Meister, [1] Glutathione metabolism, Methods Enzymol. 251 (1995) 3–7.
[71] A. Meister, M.E. Anderson, Glutathione, Annu. Rev. Biochem. 52 (1983) 711–760.
[72] B.R. You, S.H. Kim, W.H. Park, Reactive oxygen species, glutathione, and thioredoxin influence suberoyl bishydroxamic acid-induced apoptosis in A549 lung cancer cells, Tumor Biol. 36 (2015) 3429–3439.
[73] N.M. Elsayed, S.T. Omaye, Biochemical changes in mouse lung after subcutaneous injection of the sulfur mustard 2-chloroethyl 4-chlorobutyl sulfide, Toxicology 199 (2004) 195–206.
[74] M. Pohanka, R. Stetina, H. Svobodova, B. Ruttkay-Nedecky, M. Jilkova, J. Sochor, J. Sobotka, V. Adam, R. Kizek, Sulfur mustard causes oxidative stress and depletion of antioxidants in muscles, livers, and kidneys of Wistar rats, Drug Chem. Toxicol. 36 (2013) 270–276.
[75] M. Jafari, M. Ghanei, Evaluation of plasma, erythrocytes, and brochoalveolar lavage fluid antioxidant defense system in sulfur mustard-injured patients, Clin. Toxicol. 48 (2010) 184–192.
[76] M. Ghanei, M. Shohrati, M. Jafari, S. Ghaderi, F. Alaeddini, J. Aslani, N-acetylcysteine improves the clinical conditions of mustard gas-exposed patients with normal pulmonary function test, Basic Clin. Pharmacol. Toxicol. 103 (2008) 428–432.
[77] M. Shohrati, J. Aslani, M. Eshraghi, F. Alaedini, M. Ghanei, Therapeutics effect of N-acetyl cysteine on mustard gas exposed patients: evaluating clinical aspect in patients with impaired pulmonary function test, Respir. Med. 102 (2008) 443–448.
[78] N. Shangari, P.J. O'Brien, Catalase activity assays, Curr. Protoc. Toxicol. 27 (2006) 7.7.1–7.7.16.
[79] W.-H. Sun, F. Liu, Y. Chen, Y.-C. Zhu, Hydrogen sulfide decreases the levels of ROS by inhibiting mitochondrial complex IV and increasing SOD activities in cardiomyocytes under ischemia/reperfusion, Biochem. Biophys. Res. Commun. 421 (2012) 164–169.
[80] K. Husain, S.N. Dube, K. Sugendran, R. Singh, S. Das Gupta, S.M. Somani, Effect of topically applied sulphur mustard on antioxidant enzymes in blood cells and body tissues of rats, J. Appl. Toxicol. 16 (1996) 245–248.
[81] L. Mirbagheri, M.H. Roudkenar, A.A.I. Fooladi, M. Ghanei, M.R. Nourani, Downregulation of super oxide dismutase level in protein might be due to sulfur mustard induced toxicity in lung, Iran. J. Allergy, Asthma Immunol. 12 (2013) 153–160.
[82] Y. Panahi, M. Ghanei, E. Vahedi, A. Ghazvini, S. Parvin, N. Madanchi, M. Bagheri, A. Sahebkar, Effect of recombinant human IFNγ in the treatment of chronic pulmonary complications due to sulfur mustard intoxication, J. Immunotoxicol. 11 (2014) 72–77.
[83] M. Shohrati, M. Ghanei, N. Shamspour, M. Jafari, Activity and function in lung injuries due to Sulphur mustard, Biomarkers 13 (2008) 728–733.
[84] Y.-B. Kim, Y.-S. Lee, D.-S. Choi, S.-H. Cha, D.-E. Sok, Change in glutathione S-transferase and glyceraldehyde-3-phosphate dehydrogenase activities in the organs of mice treated with 2-chloroethyl ethyl sulfide or its oxidation products, Food Chem. Toxicol. 34 (1996) 259–265.
[85] M.R. Nourani, S. Azimzadeh, M. Ghanei, A.A. Imani Fooladi, Expression of glutathione S-transferase variants in human airway wall after long-term response to sulfur mustard, J. Recept. Signal Transduct. 34 (2014) 125–130.
[86] A.H. Dastjerdi, H. Behboudi, Z. Kianmehr, A. Taravati, M.M. Naghizadeh, S.K. Ardestani, T. Ghazanfari, Association of glutathione S-transferase polymorphisms with the severity of mustard lung, BioImpacts BI 7 (2017) 255.
[87] E. Lubos, J. Loscalzo, D.E. Handy, Glutathione peroxidase-1 in health and disease: from molecular mechanisms to therapeutic opportunities, Antioxid. Redox Signal. 15 (2011) 1957–1997.
[88] M. Ucar, A. Korkmaz, R.J. Reiter, H. Yaren, S. Öter, B. Kurt, T. Topal, Melatonin alleviates lung damage induced by the chemical warfare agent nitrogen mustard, Toxicol. Lett. 173 (2007) 124–131.
[89] X.-J. Zhu, R. Xu, X. Meng, H.-B. Chu, C. Zhao, C.-J. Lian, T. Wang, W.-J. Guo, S.-M. Zhang, Mechanistic insights of sulfur mustard-induced acute tracheal injury in rats, Int. J. Toxicol. 33 (2014) 382–392.
[90] I. Carlberg, B. Mannervik, [59] glutathione reductase, Methods Enzymol, Elsevier, 1985, pp. 484–490.
[91] M. Pohanka, J. Sobotka, R. Stetina, Sulfur mustard induced oxidative stress and its alteration by epigallocatechin gallate, Toxicol. Lett. 201 (2011) 105–109.
[92] S.D. Sawale, P.D. Ambhore, P.P. Pawar, U. Pathak, U. Deb, R.M. Satpute, Ameliorating effect of S-2 (ω-aminoalkylamino) alkylaryl sulfide (DRDE-07) on sulfur mustard analogue, 2-chloroethyl ethyl sulfide-induced oxidative stress and inflammation, Toxicol. Mech. Methods 23 (2013) 702–710.
[93] E. Tahmasbpour, M. Ghanei, A. Qazvini, E. Vahedi, Y. Panahi, Gene expression profile of oxidative stress and antioxidant defense in lung tissue of patients exposed to sulfur mustard, Mutat. Res. Toxicol. Environ. Mutagen. 800 (2016) 12–21.
[94] F. Cheng, M. Torzewski, A. Degreif, H. Rossmann, A. Canisius, K.J. Lackner, Impact of glutathione peroxidase-1 deficiency on macrophage foam cell formation and proliferation: implications for atherogenesis, PLoS One 8 (2013) e72063.